Contents lists available at ScienceDirect

Journal of Neuroscience Methods

A method for unit recording in the lumbar spinal cord during locomotion of the conscious adult rat

Rune W. Berg [a,*], Ming-Teh Chen [e,f], Hsueh-Chen Huang [c,d], Min-Chi Hsiao [b], Henrich Cheng [c,d,g,h]

[a] *Department of Neuroscience and Pharmacology, 12.5.5, University of Copenhagen, Blegdamsvej 3, DK-2200, Copenhagen N, Denmark*
[b] *Department of Biomedical Engineering, University of Southern California, Los Angeles, CA, USA*
[c] *Division of Neural Regeneration Laboratory, Department of Neurosurgery, Neurological Institute, Taipei Veterans General Hospital, Taiwan*
[d] *Center for Neural Regeneration, Department of Neurosurgery, Neurological Institute, Taipei Veterans General Hospital, Taiwan*
[e] *Department of Surgery, School of Medicine, National Yang Ming University, Taipei, Taiwan*
[f] *Department of Neurosurgery, Neurological Institute, Taipei Veterans General Hospital, Taiwan*
[g] *Department & Institute of Pharmacology, School of Medicine, National Yang-Ming University, Taipei, Taiwan*
[h] *Faculty of Medicine, School of Medicine, National Yang-Ming University, Taipei Taiwan*

ARTICLE INFO

ABSTRACT

Extracellular recordings from single units in the brain, for example the neocortex, have proven feasible in moving, awake rats, but have not yet been possible in the spinal cord. Single-unit activity during locomotor-like activity in reduced preparations from adult cats and rats have provided valuable insights for the development of hypotheses about the organization of functional networks in the spinal cord. However, since reduced preparations could result in spurious conclusions, it is crucial to test these hypotheses in animals that are awake and behaving. Furthermore, unresolved issues such as how muscle force precision is achieved by motoneurons as well as how spinal neurons are spatio-temporally correlated are better to investigate in the conscious and behaving animal. We have therefore developed procedures to implant arrays of extracellular recording electrodes in the lumbar spinal cord of the adult rat for long-term studies. In addition, we implanted pairs of electromyographic electrodes in the hindlimbs for the purpose of monitoring locomotion. With our technique, we obtained stable long-term recordings of spinal units, even during locomotion. We suggest this as a novel method for investigating motor pattern-generating circuitry in the spinal cord.

© 2009 Elsevier B.V. All rights reserved.

1. Introduction

It is well established that the local circuitry in the lumbar portion of the spinal cord generates rhythmic motor behaviors (Bizzi et al., 1995; Grillner, 2006) such as scratching (Berkinblit et al., 1978; Berkowitz, 2002; Stein, 2005; Stein et al., 1998), swimming (Berkowitz, 2005) and walking (Kiehn, 2006). The locomotor-related circuitry is distributed in the ventromedial region of the lumbar segments of the spinal cord (Cazalets et al., 1996; Cowley and Schmidt, 1997; Deliangina et al., 1983; Kjaerulff and Kiehn, 1996; Orlovsky et al., 2003; Tresch and Kiehn, 1999). Neural activity of rhythmic movements has been studied extensively in fictive locomotion in *in vitro* preparations and has been complemented with studies on functional electrical stimulation in the motor nuclei

(Saigal et al., 2004; Tresch and Bizzi, 1999) and recordings from the dorsal root ganglia (Ayoyagi et al., 2003; Baker et al., 2006; Fetz et al., 2002; Weber et al., 2006) of monkey and cat. In spite of this, reports from awake and locomoting animals are missing (Orlovsky et al., 2003). In analogy with observations in the neocortex (Holt et al., 1996), fundamental differences most likely exist between pharmacologically induced activity in the developing/immature spinal cord *in vitro* compared with real movements in the adult, conscious animal *in vivo*. Furthermore, issues such as neural control of muscle force (Bizzi et al., 2008) and precision of force, as well as spatio-temporal correlations of activity (Tresch and Kiehn, 2002) are expected to be more pronounced in the awake animal. In spite of this and recent advances in large-scale recordings and neural prosthetics (Churchland et al., 2007; Hochberg et al., 2006; Schwartz et al., 2006), investigators of functional spinal circuitry have been reluctant to pursue these types of experiments since conscious animals generate movements that may interfere with the recording. We have therefore developed a technique that involves implanting
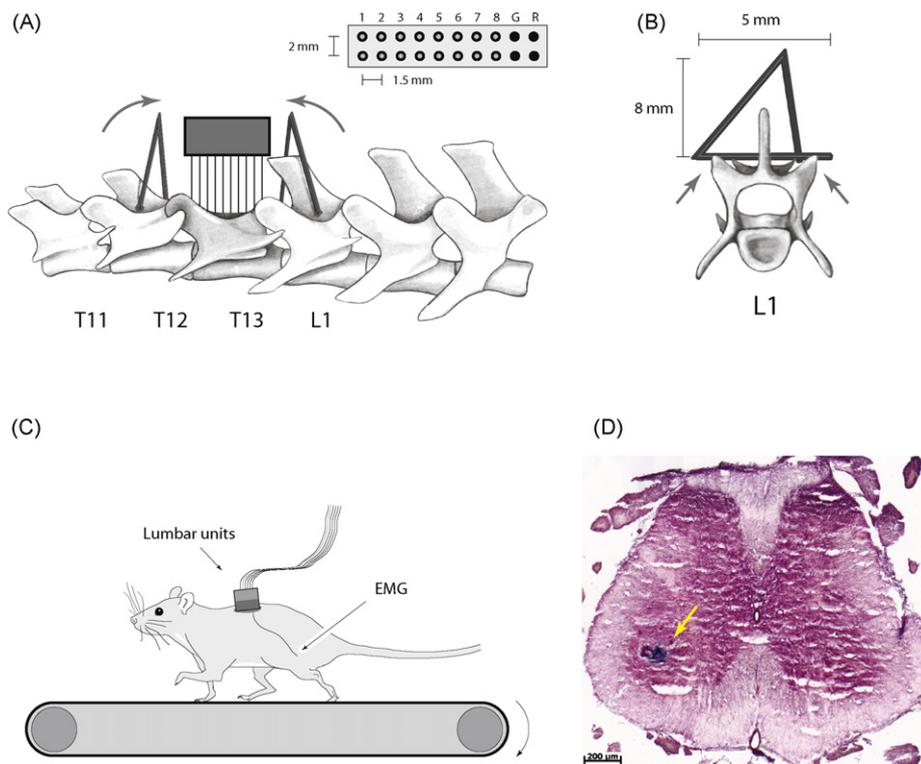
Fig. 1. Illustration of implantation and setup. (A) Sagittal view of lower thoracic and lumbar vertebrae. An adapted triangular steel wire was inserted in vertebrae T12 and L1, rotated in the direction of the arrows and glued with super glue. The 16-electrode array was inserted into the spinal segment of vertebra T13. The inset illustrates the 16-electrode array, including 2 ground and 2 reference electrodes. The electrode tips were at an equal depth of 1–2 mm from the surface. (B) Transverse view of the L1 vertebra illustrating the geometry and insertion of the steel triangle. The arrows show the lateral points of support for the steel wire. Vertebra figure adapted from (Popesko et al., 2003). (C) Illustration of the recording session in which the EMG output is combined with the multi-unit readings from the lumbar spinal cord. (D) Histological sample showing the lesion marks of an electrode in the ventral horn in L4 (yellow arrow, animal 322).

and anchoring extracellular multi-unit recording arrays in conjunction with electro-myographic (EMG) electrodes in the limb muscles. The term "multi-units" refers to multiple single units. A single unit is a representation of a putative neuron or a small group of neurons firing together in a point-like manner, i.e., a "single unit" (Buzsaki, 2004; Lewicki, 1998). We chose the lower lumbar spinal cord for the prospect of recording locomotor-related neural unit activity (Orlovsky et al., 2003; Puskar and Antal, 1997), but the technique should, in principle, work with most of the lumbar vertebrae with spinal processes.

2. Materials and methods

2.1. Animals

Six adult female rats (Sprague–Dawley, 280–290 g) were used for this study. All animals were kept in a ventilation-, humidity-, and temperature-controlled setting with a 12/12 h light/dark cycle. Rats were individually housed in clear polycarbonate cages with access to food pellets and water. The experimental procedures and treatment of rats were in accordance with Taiwanese laws governing the protection of animals used for experimental purposes.

2.2. Chronic microelectrode implantation

The animals were transferred from their cages to an air-tight container with a continuous flow of air mixed with isoflurane. When they were fully anesthetized, they were then placed on a heating pad. Anesthesia was maintained by inhalation of air mixed with isoflurane delivered through a nozzle, which was fitted to the nose. The amount of isoflurane was adjusted appropriately

throughout the surgery to be between 0 and 3%, depending on the strength of the pinna reflex. The fur was shaved above vertebra T12, the area was cleaned carefully with surgical scrub and an incision was made along the length of the vertebrae. The last rib was identified as the index of T12, and the muscle tissue surrounding T11–L3 was removed with bone scissors until the vertebral joints were visible. The T11–L3 vertebral column was held in place with tightened transverse process clamps (Cunningham Spinal Adaptor, Stoelting Co.). Two transverse holes (outer diameter > 1 mm) were drilled with a dental drill (burr size 1/4 in.) through the dorsal spinal process of the T12 and L1 vertebrae so the stainless steel wire could fit through (Fig. 1A). Two pieces of stainless steel wire (3 cm in length, 1 mm in diameter, Ethicon steel wire monofilament (CrNi) non-absorbable suture (TR-55)) were bent into an open triangular shape. One end was inserted through the hole and the triangle was rotated towards the probe (see arrows, Fig. 1A) so the other open end rested on the vertebra. The triangles were then temporarily glued with superglue (cyanoacrylate, 405 Loctite). This positioning served the purpose of preventing rostro-caudal movement of the implantation, thereby stabilizing the recording of units. Similarly, lateral movement was prevented by letting the steel wires rest on the bone on both sides of the midline process (see arrows, Fig. 1B). After inserting the electrodes, the steel wires were further anchored with dental cement (see below) so that the stable positions of the wire triangles became permanent. Finally, the electrode implant, the stainless steel triangles and the exposed vertebrae were encapsulated in dental cement with connectors protruding.

The L4–L5 spinal segments were exposed after laminectomy. Due to differential development of the spinal cord and vertebrae, the L4–L5 segments of the spinal cord are located beneath the T13–L1 vertebrae (Gelderd and Chopin, 1977). Two sagittal incisions

Table 1

The number of detected units in each of the four animals on a given day after surgery. Spike sorting and recording were done in a 30 min recording session on the given day. The first number is the total number of units, whereas the second number refers to a subset of rhythmic units (hence the "R").

Animal number	Day after surgery											Average units/day
	1	2	3	4	5	6	7	8	12	14	19	
314					9, 3R	4, 3R	5, 4R		3, 1R			5.25
322				5	4			5			1R	3.75
327	7	6	9, 5R							1		5.75
328		5, 1R								1		3.0

1 mm apart from the central vessel were made on the dura with a sterile 25-gauge needle to make room for the recording electrodes. The electrode arrays consisted of 16 insulated stainless steel wires (50 μm in diameter, NB Labs, Denison, TX). The arrays were fixed to a stereo-taxic manipulator and manually lowered to a 1–2 mm depth from the surface cord area. One stainless steel ground wire was gently inserted 1–2 mm ventrally into the posterior ipsilateral lumbar cord. The arrays were mounted to the steel pins with bone cement (Osteobond, Zimmer) to form a solid arthrodesis between the vertebrae. The locations of the electrodes were assumed to remain stable throughout the experiments and post-mortem histology was performed to inspect the vestiges (Fig. 1).

2.3. Implantation of EMG electrodes

Five pieces of 15-cm long microwire with Teflon insulation (50 μm; No. 7955, A-M Systems) were adapted to the purpose of surgical implantation and monitoring of conglomerate muscle activity in a fashion similar to that previously described (Berg et al., 2005). A small incision in the skin was made above the hindlimb thigh muscle (*m. rectus femoris*), and the tissue was expanded and held with sutures. A spinal syringe needle (Terumo corporation, Tokyo Japan, gauge 23Gx3 1/2 (0.65 mm × 90 mm)) was pushed through the connective tissue under the skin from the incision up to the area of the spinal cord, where the implantation was located (see above). The five microwires were then channeled through the syringe and the syringe was carefully withdrawn, leaving the wires under the skin. The tips of the wires were stripped of ~1 mm of insulation and bent to form a hook. This hook was carefully inserted into the hindlimb thigh muscle (*m. rectus femoris*), and the wires were mounted to the muscle with silk sutures (size 5-0). The wires were curved into a semi-circle to allow room for leg movement and to prevent the wires from coming out of the muscle during locomotion. The fifth wire served as a grounding reference and was left dorsally in the connective tissue in the back above the vertebrae. All wires were soldered to a 10-pin connector next to the implantation (Fig. 1). The skin was then closed around the implant. Subjects were allowed 1–2 days to recover from this surgical procedure. Neomycin was applied to the wound and antibiotics (Borgal, Hoechst; 100 ml containing sulfadoxin 20 mg, trimethoprim 4 mg, sodium hydroxide 2.65 mg, diaethanolamine 0.3 mg, glycerinoformal 76.65 mg) at a dosage of 1.5 mg/100 g were injected subcutaneously once daily for the first 7 days to prevent infection.

2.4. Electrophysiology

The microelectrode was affixed to the thoracic vertebrae such that a plug at the end of the arrays remained accessible for connection to the recording apparatus via a headset cable (Fig. 1C) that also connected to a commutator (Drangonfly Inc.) in the ceiling of the experimental chamber. Neural signals corresponding to extracellularly measured action potentials were conditioned via field effect transistors embedded within the headset plug and were amplified, filtered, digitized and sorted online using a 16-channel neuron recording system (Plexon Inc., Dallas, TX) (Chen et al., 2001). The

waveforms and their time of occurrence were selected based upon waveform amplitude and shape and saved (Fee et al., 1996; Shoham et al., 2003) (see Section 2.6). The recording continued while the animal was either running or walking on a treadmill (Stoelting, Wood Ale IL, USA, Cat. No. 58706). The treadmill belt area was 50 cm long and 25 cm wide. The speed of the treadmill was kept between 5 and 15 cm/s. A recording session lasted approximately 30 min and consisted of both template formation for spike sorting and actual recording. The animal was allowed occasional breaks. The spike waveform templates were kept and used during the next recording session, which was typically 2–3 days later (see Table 1), though they often had to be adapted. Continual recording never exceeded 30 min. The rat spent the time between recording sessions in its cage in the vivarium.

2.5. Histology

At the end of the experimental period, animals were deeply anesthetized with sodium pentobarbital (6.5 mg/100 g), and the location of the tips of all wires marked by applying approximately 10 μA of constant positive current, which deposited Fe^{2+} into the tissue. Using a pump, animals were perfused transcardially. At the beginning of the perfusion, the perfusion medium consisted of 300 ml 37 °C 0.1 M PB (NaH_2PO_4 8.415 g and NaOH 1.925 g in 0.5 l distilled water). Then, the medium was replaced with 300 ml of 4% paraformaldehyde solution (NaOH 1.925 g, paraformaldehyde 20 g and NaH_2PO_4 8.415 g in 0.5 l distilled water) as described (Berg et al., 2006; Cheng et al., 1996; Cheng and Olson, 1995). Finally, the perfusion medium was exchanged with a solution containing 200 ml of 3% potassium ferrocyanide/4% paraformaldehyde solution to fix the tissue and to form a blue reaction product at the site of iron deposition. Following perfusion, the spinal cord was transferred and kept in a 4% paraformaldehyde solution overnight. The following day, the tissue was rinsed three times in phosphate buffered saline, with each rinse lasting 30 min. Then, the tissue was rinsed in phosphate buffered saline containing 18% sucrose for 30 min and finally transferred to a solution of 18% sucrose in distilled water and kept there for 1 day. The spinal tissue containing the implantation site was blocked with tissue freezing medium and sectioned using a cryostat (Leica Microsystems, model CM3050, Mannheim Germany). The tissue was sliced in 50-μm coronal sections and mounted on glass slides. Samples were inspected under a microscope (Zeiss Axiophots, Germany) and photographed with a high-resolution digital camera (Zeiss, Axio Cam HRc, Germany). The electrode tracks and blue reaction products were visible in these histological preparations, allowing for verification of the location of the microwire electrode tips. There were 8 equally spaced electrodes (1.5 mm apart) in the left and the right side in each animal (16 total) spanning the region between L4 and L5, aimed at the ventral part of the horns (laminae VIII–IX) (see Fig. 1). Confirmed locations of the lesions were: rat 322: 3 in IX L4, 5 in IX/white matter borderline; rat 327: all 16 electrodes in the ventro-lateral white matter L5; and for rat 328: 8 lesions were found in the ventro-lateral white matter. Rat 314 died prematurely, and the histological procedure could not be performed.
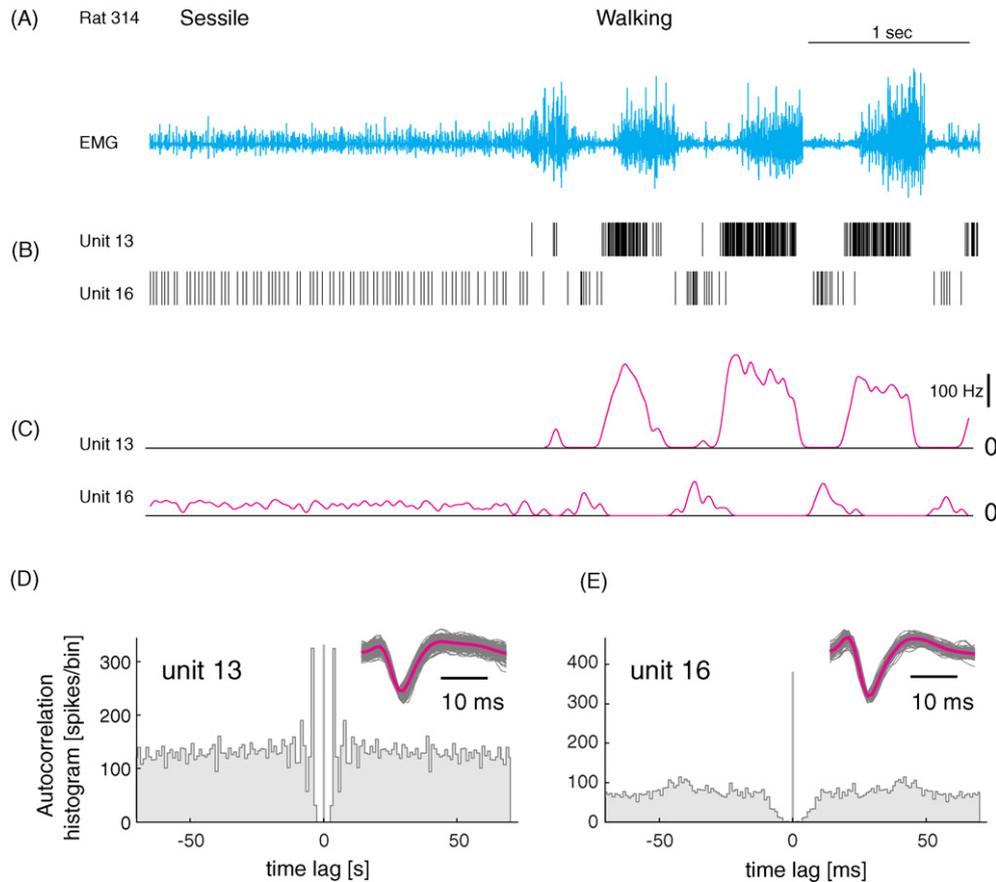
Fig. 2. From stance to walking. (A) EMG recording from the left thigh (*m. rectus femoris*) during a transition from stillness to walking. (B) Concurrent activity of two single units from the left ventral lumbar spinal cord. (C) The spiking rate was estimated using the two units in (B) and a Gaussian filter. (D and E) The autocorrelation histogram of the two units (insets, with red as the average) ensures proper spike sorting.

2.6. Data analysis

Data acquisition and spike sorting were performed using the software tool RASPUTIN (real-time acquisition system programs for unit timing in neuroscience), which is a semi-manual spike-sorting platform that comes with Plexon multi-channel acquisition hardware (Plexon Inc., Texas). The sorting of single units consisted of several steps (Brown et al., 2004). First, the candidate waveforms of extracellular action potentials were triggered by a manually chosen threshold, collected and aligned for comparison. From these candidates, a template was selected by visual inspection of cluster-separation in a parameter space whose dimensions were severely reduced via principal component analysis. Each template was a reflection of a putative neuron or a small group of neurons firing together in a point-like manner, i.e., a "single unit" (Buzsaki, 2004; Lewicki, 1998). After template selection, new data were acquired and compared with the templates. Since neurons have refractory periods, the main criterion for verification of successful isolation of single units was that the autocorrelation histogram of the inter-spike intervals went to zero for time lags close to the origin (Fee et al., 1996; Lewicki, 1998) (Fig. 2D and E). For successfully identified units, a time-stamp was assigned to the peak of the waveform that indicated the time of occurrence (Figs. 2B and 3B).

Data from individual sessions were imported into the software called Neuroexplorer (Plexon Inc.) for offline analysis. Data analysis for selected animals was performed in Matlab (version 7.3, Mathworks) with custom designed software procedures. The time-
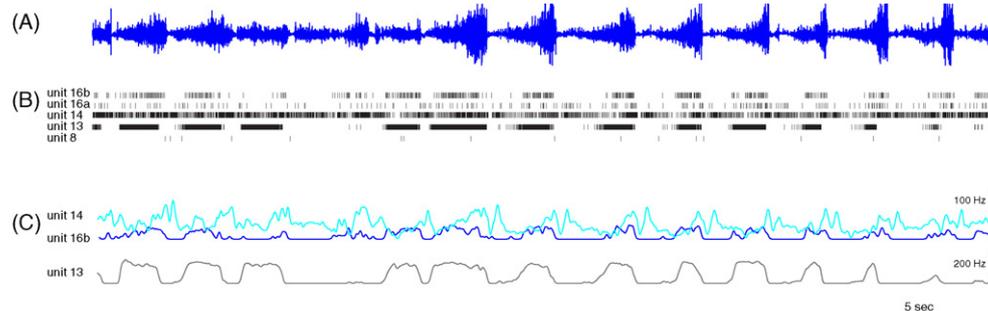

Fig. 3. Correlation among units during locomotion. (A) EMG recording from the left thigh (*m. rectus femoris*) during walking. (B) The concurrent activity of 5 units from the left ventral lumbar spinal cord. (C) The estimated spike rate using a Gaussian kernel for the three most rhythmic units, units 13, 14 and 16b. Data from rat 314.
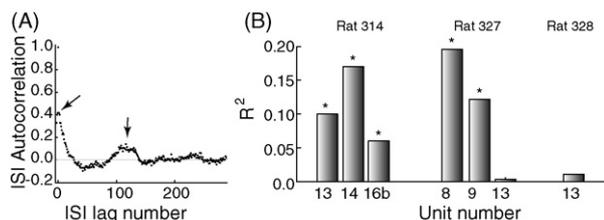
Fig. 4. Spike pattern statistics. (A) The autocorrelation of the inter-spike intervals as a function of number of lags of unit 14 ($R^2 = 0.17$ for lag = 1, *see left arrow*). The second peak represents the average number of ISIs on repetition into the next cycle (~120 spikes/burst, *see right arrow*). (B) The R^2 values for all rhythmic units. Significant autocorrelations are marked with an asterisk (*) (95% confidence).

dependent firing rate shown in Figs. 2 and 3 was estimated using binning and Gaussian kernel filtering (Dayan and Abbott, 2005).

3. Results

3.1. Spike patterns

Four out of six rats had successful implantation of both EMG electrodes and extracellular spinal electrodes, which collected spinal unit activity. Of the two unsuccessful rats, one died from the surgery. For unknown reasons, we were unable to record unit activity from the spinal electrodes of the second rat. Out of the 16 electrodes implanted in each successful animal, there was an average of 4.4 units on a given recording day (see Table 1). Some units were silent during resting and active during locomotion (9%, 6/65 units) while other units were tonically active at rest and became modulated during locomotion (11%, 7/65 units). We defined locomotor-related unit activity as activity having correlation with the rhythmic EMG, and we monitored this activity during treadmill locomotion (Leblond et al., 2003). A majority of the units (80%, 52/65 units) were not active in any obvious relation with the locomotion, though we cannot exclude the possibility that they were part of a population activity (Shadlen and Newsome, 1998) related to locomotion.

A rat running on the treadmill would not run at a continuous pace, but instead performed bouts of running interrupted by brief static postures for 1–2 s, depending on the speed of the treadmill. During these quiet postures, the EMG showed muscle tone and certain units (11%, 7/65 units) would be constantly active. The same units showed bursting during locomotion (Fig. 2A–C). The criterion for selecting a unit was that the autocorrelation histogram had no events close to zero, which assured that they had refractory periods (Fig. 2D and E). Another set of sample data is shown in Fig. 3. The units were stable and kept throughout the recording session. The templates were stored for later sessions, though new templates often had to be formed during a later recording session.

3.2. Irregularity of spiking

We looked at the pattern of spiking in the rhythmic units (i.e., the units that were directly related to walking for the purpose of determining their irregularity. The autocorrelation among consecutive inter-spike intervals is an easy means of estimating the degree of irregularity of spiking (Berg et al., 2007; Calvin and Stevens, 1968) when the spiking is non-stationary and the coefficient of variation of ISIs does not apply. The autocorrelation function for increasing shifts in ISI number indicates both long-term recurrent patterns as well as immediate regularity in modulation (Tuckwell, 1988). Even though the stepping cycle was variable, a smaller, second peak was visible in the ISI-autocorrelation histogram, representing the average number of spikes per burst (right arrow, Fig. 4A). We

also observed a small but significant correlation among the nearest neighbor ISI (left arrow in Fig. 4A) in 5 out of 7 units recorded from three animals (Fig. 4B).

3.3. Number of spikes per burst

If a rhythmic firing rate modulation were present, it would manifest itself as a second peak in the autocorrelation histogram (Fig. 4A) where its significance would be established by the regular correlation coefficient procedure (Taylor, 1982). The number of spikes per cycle could then be estimated as the location of the second peak in the ISI-autocorrelation sequence (right arrow in Fig. 4A). The mean across 7 units was 55 spikes/burst with a standard deviation of 40 spikes/burst. These numbers are fairly high compared with neonatal *in vitro* measurements of 4–5 spikes per cycle (Raastad and Kiehn, 2000), but they are not unreasonable compared with motor-unit recordings from awake adult rats (Gorassini et al., 2000).

4. Discussion

In the present study we have developed a technique for anchoring extracellular recording arrays to the lumbar vertebrae with the purpose of recording, over the long term, spinal units in conjunction with limb EMG recordings during locomotion (Fig. 1). To our knowledge, this is the first report on neuronal activity in the lumbar spinal cord of the adult rat, awake and moving of its own volition.

When on the treadmill, the rat ran or walked in short bouts interlaced with breaks (Fig. 2). During movement bouts, the EMG signals had clear rhythmic activity, which we used to identify units directly related to locomotion in the lumbar spinal cord. The number of spikes per cycle of these units was higher than those reported in, for example, neonatal preparations (Tresch and Kiehn, 1999). Similarly, the firing peak frequency during a burst was as high as 200 Hz during locomotion of the awake adult, whereas the peak frequencies reported in pharmacologically induced fictive locomotion in the neonatal rat is below 10 Hz (Raastad and Kiehn, 2000). However, the peak frequency of units recorded in the muscles in adult awake rats (Gorassini et al., 2000) and in motoneurons in adult turtles (Berg et al., 2007; Berg et al., 2008) are more than 100 Hz, which are comparable to our observed frequencies. Nevertheless, the findings in the present study are based on a small sample, so it is not possible at this point to make a general conclusion about firing frequency and number of spikes per cycle. Our main result is that *in vivo* recording from awake rats is possible and can be stable throughout a recording session.

This multi-unit recording technique is an important tool for investigating issues such as spatial and temporal correlation among interneurons and motoneurons, which could lead to improved research on pathological conditions such as tremor (Tresch and Kiehn, 2002), spinal seizure and myoclonus. Seizure and tremor are manifestations of excessive neuronal synchronization (Kandel et al., 1991). Therapeutic strategies, such as localization of the seizure source and assessment of neuronal couple strength in response to pharmacological agents, require continuous unit recording from multiple sites. Furthermore, recording from multiple units is essential for establishing differences such as the degree of "rate-code" versus "time-code" (Berg et al., 2008; Konig et al., 1996) in spinal motor function. In a rate-coding scheme, the spike times of individual neurons will have no significant correlation, while in a time-coding scheme they will. The timescale of this correlation will be much shorter than the timescale of the motor behavior itself (Theunissen and Miller, 1995). The rigid definition proposed by Theunissen and Miller states that if the encoding of a sensory signal, which has been decomposed into Fourier spectral components, has significant components higher than

the frequency cut-off of sensation then it is a temporal encoding. On the contrary, if there is no correlation between these higher order kernels of the signal and the spike times, then the sensory information is represented as a rate encoding.

Multi-unit recording also allows experimental distinction between two types of dynamic processes within the motor pattern circuitry. One is a process in which the bursts are distributed over a population of interneurons (Shadlen and Newsome, 1998) and in which each interneuron only participates with between less than one or only a few spikes per cycle. An alternative process could be a strict modular arrangement with fewer, albeit more directly participating interneurons (Pearson, 2000). The multi-unit recording technique presented in this study is an important tool for investigating these issues as well as for verifying findings from reduced preparations. Though the technique is invasive, it represents an electrophysiological preparation, which is currently the closest to the intact animal. It is thus feasible, with this relatively simple procedure, to verify findings from previous reduced preparations, for example the pharmacologically activated fictive locomotion in spinal segments of neonatal rat, on conscious adult animals moving of their own volition.

Acknowledgements

References

Ayoyagi Y, Stein RB, Branner A, Pearson KG, Normann RA. Capabilities of a penetrating microelectrode array for recording single units in dorsal root ganglia of the cat. J Neurosci Meth 2003;128:9–20.

Baker SN, Chiu M, Fetz EE. Afferent encoding of central oscillations in the monkey arm. J Neurophysiol 2006;95:3904–10.

Berg RW, Alaburda A, Hounsgaard J. Balanced inhibition and excitation drive spike activity in spinal half-centers. Science 2007;315:390–3.

Berg RW, Ditlevsen S, Hounsgaard J. Intense synaptic activity enhances temporal resolution in spinal motoneurons. PLoS ONE 2008;3(9):e3218.

Berg RW, Friedman B, Schroeder LF, Kleinfeld D. Activation of nucleus basalis facilitates cortical control of brain stem motor programs. J Neurophysiol 2005;94:699–711.

Berg RW, Whitmer D, Kleinfeld D. Exploratory whisking by rat is not phase locked to the hippocampal theta rhythm. J Neurosci 2006;26:6518–22.

Berkinblit MB, Deliagina TG, Feldman AG, Gelfand IM, Orlovsky GN. Generation of scratching. I. Activity of spinal interneurons during scratching. J Neurophysiol 1978;41:1040–57.

Berkowitz A. Both shared and specialized spinal circuitry for scratching and swimming in turtles. J Comp Physiol A 2002;188:225–34.

Berkowitz A. Physiology and morphology indicate that individual spinal interneurons contribute to diverse limb movements. J Neurophysiol 2005;94:4455–70.

Bizzi E, Cheung VCK, d'Avella A, Saltiel P, Tresch M. Combining modules for movement. Brain Res Rev 2008;57:125–33.

Bizzi E, Giszter SF, Loeb E, Mussa-Ivaldi FA, Saltiel P. Modular organization of motor behavior in the frogs spinal cord. Trends Neurosci 1995;18:442–6.

Brown EN, Kass RE, Mitra PP. Multiple neural spike train data analysis: state-of-the-art and future challenges. Nat Neurosci 2004;7:456–61.

Buzsaki G. Large-scale recording of neuronal ensembles. Nat Neurosci 2004;7:446–51.

Calvin WH, Stevens CF. Synaptic noise and other sources of randomness in motoneuron interspike intervals. J Neurophysiol 1968;31:574–87.

Cazalets JR, Borde M, Clarac F. Localization and organization of the central pattern generator for the hindlimb locomotion in newborn rat. J Neurosci 1996;15:4943–51.

Chen MT, Morales M, Woodward DJ, Hoffer BJ, Janak PH. In vivo extracellular recording of striatal neurons in the awake rat following unilateral 6-hydroxydopamine lesions. Exp Neurol 2001;171:72–83.

Cheng H, Cao Y, Olson L. Spinal cord repair in adult paraplegic rats: partial restoration of hind limb function. Science 1996;273:510–3.

Cheng H, Olson L. A new surgical technique that allows proximodistal regeneration of 5-HT fibers after complete transection of the rat spinal cord. Exp Neurol 1995;136:149–61.

Churchland MM, Yu BM, Sahani M, Shenoy KV. Techniques for extracting single-trial activity patterns from large-scale neural recordings. Curr Opin Neurobiol 2007;17:609–18.

Cowley KC, Schmidt BJ. Regional distribution of the locomotor pattern-generating network in the neonatal rat spinal cord. J Neurophysiol 1997;77:247–59.

Dayan P, Abbott LF. Theoretical neuroscience: computational and mathematical modeling of neural systems. paperback ed. MIT Press; 2005.

Deliangina TG, Orlovsky GN, Pavlova GA. The capacity for generation of rhythmic oscillation is distributed in the lumbosacral spinal cord of the cat. Exp Brain Res 1983;53.

Fee MS, Mitra PP, Kleinfeld D. Automatic sorting of multiple unit neuronal signals in the presence of anisotropic and non-Gaussian variability. J Neurosci Meth 1996;69:175–88.

Fetz EE, Perlmutter SI, Prut Y, Seki K, Votaw SS. Roles of primate spinal interneurons in preparation and execution of voluntary hand movement. Brain Res Rev 2002;40:53–65.

Gelderd JB, Chopin SF. The vertebral level of origin of spinal nerves in the rat. Anat Rec 1977;188:45–8.

Gorassini M, Eken T, Bennett DJ, Kiehn O, Hultborn H. Activity of hindlimb motor units during locomotion in the conscious rat. J Neurophysiol 2000;83:2002–11.

Grillner S. Biological pattern generation: the cellular and computational logic of networks in motion. Neuron 2006;52:751–66.

Hochberg LR, Serruya MD, Friehs GM, Mukand JA, Saleh M, Caplan AH, et al. Neuronal ensemble control of prosthetic devices by a human with tetraplegia. Nature 2006;442:164–71.

Holt GR, Softky WR, Koch C, Douglas RJ. Comparison of discharge variability in vitro and in vivo in the cat visual cortex neurons. J Neurophysiol 1996;75:1806–14.

Kandel ER, Schwartz JH, Jessell TM. Principles of neural science. Appleton and Lange; 1991.

Kiehn O. Locomotor circuits in the mammalian spinal cord. Annu Rev Neurosci 2006;29:279–306.

Kjaerulff O, Kiehn O. Distribution of networks generating and coordinating locomotor activity in the neonatal rat spinal cord in vitro: a lesion study. J Neurosci 1996;16:5777–94.

Konig P, Engel AK, Singer W. Integrator or coincidence detector? The role of the cortical neuron revisited. TINS 1996;19:130–7.

Leblond H, L'Esperance M, Orsal D, Rossignol S. Treadmill locomotion in the intact and spinal mouse. J Neurosci 2003;23:11411–9.

Lewicki MS. A review of methods for spike sorting: the detection and classification of neural action potentials. Network: Comput Neural Syst 1998;9:R53–78.

Orlovsky GN, Deliagina TG, Grillner S. Neuronal control of locomotion—from mollusc to man. Oxford University Press; 2003.

Pearson KG. Neural adaptation in the generation of rhythmic behavior. Annu Rev Physiol 2000;62:723–53.

Popesko P, Rajtova V, Horak J. A colour atlas of anatomy of small laboratory animals, vol. 256. Saunders Ltd; 2003.

Puskar Z, Antal M. Localization of last-order premotor interneurons in the lumbar spinal cord of rats. J Comp Neurol 1997;389:377–89.

Raastad M, Kiehn O. Spike coding during locomotor network activity in ventrally located neurons in the isolated spinal cord from neonatal rat. J Neurophysiol 2000;83:2825–34.

Saigal R, Renzi C, Mushahwar K. Intraspinal microstimulation generates functional movements after spinal-cord injury. IEEE Trans Neural Syst Rehabil Eng 2004;12:430–40.

Schwartz AB, Cui XT, Weber DJ, Moran DW. Brain-controlled interfaces: movement restoration with neural prosthetics. Neuron 2006;52:205–20.

Shadlen MN, Newsome WT. The variable discharge of cortical neurons: implications for connectivity, computation, and information coding. J Neurosci 1998;18:3870–96.

Shoham S, Fellows MR, Normann RA, Robust. automatic spike sorting using mixtures of multivariate t-distributions. J Neurosci Meth 2003;127:111–22.

Stein PSG. Neuronal control of turtle hindlimb motor rhythms. J Comp Physiol A: Neuroethol Sensory Neural Behav 2005;191:213–29.

Stein PSG, McCullough ML, Currie SN. Spinal motor patterns in the turtle. Ann NY Acad Sci 1998;860:142–54.

Taylor JR. An introduction to error analysis—the study of uncertainties in physical measurements. California: University Science Books; 1982.

Theunissen F, Miller JP. Temporal encoding in nervous system: a rigorous definition. J Comput Neurosci 1995;2:149–62.

Tresch MC, Bizzi E. Responses to spinal microstimulation in the chronically spinalized rat and their relationship to spinal systems activated by low threshold cutaneous stimulation. Exp Brain Res 1999;129:401–16.

Tresch MC, Kiehn O. Coding of locomotor phase in populations of neurons in rostral and caudal segments of the neonatal rat lumbar spinal cord. J Neurophysiol 1999;82:3563–74.

Tresch MC, Kiehn O. Synchronization of motor neurons during locomotion in the neonatal rat: predictors and mechanisms. J Neurosci 2002;22:9997–10008.

Tuckwell HC. Introduction to theoretical neurobiology: nonlinear and stochastic theories. Cambridge University Press; 1988.

Weber DJ, Stein RB, Everaert DG, Prochazka A. Decoding sensory feedback from firing rates of afferent ensembles recorded in cat dorsal root ganglia in normal locomotion. IEEE Trans Neural Syst Rehabil Eng 2006;14:240–3.